

Water between Plates in the Presence of an Electric Field in an Open System[†]Subramanian Vaitheeswaran,^{‡,§} Hao Yin,^{||} and Jayendran C. Rasaiah^{*,||}

Department of Physics and Astronomy and Department of Chemistry, University of Maine, Orono, Maine 04469

Received: September 28, 2004; In Final Form: November 17, 2004

Molecular dynamics simulations of water at 298 K and 1 atm of pressure are used to investigate the electric-field dependence of the density and polarization density of water between two graphite-like plates of different sizes (9.8×9.2 and 17.7×17.2 Å) in an open system for plate separations of 8.0, 9.5, and 16.4 Å. The interactions with water were tuned to “hard-wall-like” and “normal” C–O hydrophobic potentials. Water between the larger plates at 16.4 Å separation is layered but is metastable with respect to capillary evaporation at zero field (Bratko, D.; Curtis, R. A.; Blanch, H. W.; Prausnitz, J. M. *J. Chem. Phys.* **2001**, *115*, 3873). Applying a field decreases the density of the water between the plates, in apparent contradiction to thermodynamic and integral equation theories of bulk fluid electrostriction that ignore surface effects, rendering them inapplicable to finite-sized films of water between hydrophobic plates. This suggests that the free energy barrier for evaporation is lowered by the applied field. Water, between “hard-wall-like” plates at narrower separations of 9.5 Å and less, shows a spontaneous but incomplete evaporation at zero field within the time scale of our simulation. Evaporation is further enhanced by an electric field. No such evaporation occurs, on these time scales, for the smaller plates with the “hard-wall-like” potential at a separation of 8.0 Å at zero field, signaling a crossover in behavior as the plate dimension decreases, but the water density still diminishes with increasing field strength. These observations could have implications for the behavior of thin films of water between surfaces in real physical and biological systems.

I. Introduction

A confined liquid has properties very different from those of the bulk. In small quantities, only a few molecules across, the discrete nature of matter becomes important and continuum descriptions are no longer adequate. One manifestation of this is the molecular layering observed in the classic experiments of Horn and Israelachvili.^{2–4} Another is the water occupancy of nonpolar cavities⁵ and carbon nanotubes.^{6–12} In a seminal paper, Stillinger¹³ suggested that hydrogen bonding between water molecules is partially disrupted near a hydrophobic surface, inducing dewetting. This could lead to the evaporation of a narrow film of water confined between the plates and has been the subject of many theoretical^{14–16} and computational studies.^{1,14,17–28} It has been suggested that it may also lead to attraction between two hydrophobic plates.^{4,15,20,29}

In this paper we discuss molecular dynamics (MD) simulations to study electric-field effects on water between two plates in an open system. Svischev and Kusalik³⁰ and Xia and Berkowitz³¹ have reported electric-field-induced freezing of water in MD simulations, and Yeh and Berkowitz³² studied the effect of electric fields on the dielectric constant of water between plates. They observed no perceptible change in the density of the water layers confined between two Ag(1,1,1) plates when a constant electric field of 2.5 V/Å was applied.³³

Removing one of the plates, to soften the effect of confinement, produced no significant change in the density of water near the remaining plate from which an exponentially decaying electric field emerged.³³ Zhu and Robinson³⁴ also studied water between plates in the presence of an electric field and concluded that the breakage of hydrogen bonds near the walls was enhanced by the field because of molecular alignment. These simulations were carried out in closed systems. Our observations of the behavior of water between plates in an open system are strikingly different. We find that an electric field decreases the density of a narrow film of water several angstroms wide between plates open to a reservoir. This is the opposite of what is predicted from the bulk thermodynamics of electrostriction when surface effects are ignored and, to our knowledge, has not been reported before.

The thermodynamics of a dielectric bulk fluid open to a reservoir^{35–37} and subject to an external electric field predicts that the change in density ρ with the field E is given by^{35,37}

$$\frac{1}{\rho} \left(\frac{\partial \rho}{\partial E} \right)_{\mu, V, T} = \left(\frac{\partial \mathcal{P}}{\partial P} \right)_{E, N, T} = \kappa_T \rho \left(\frac{\partial \mathcal{P}}{\partial \rho} \right)_{E, T} \quad (1)$$

where \mathcal{P} is the polarization density, P is the pressure, and κ_T $[(1/\rho)(\partial \rho / \partial P)_{E, T}]$ is the compressibility of the fluid at a volume V , a temperature T , and a chemical potential μ . The temperature and chemical potential are identical to those of the reservoir which is in thermal and chemical equilibrium with the dielectric fluid. Combining this with the linear constitutive relation

$$\mathcal{P} = \left(\frac{\epsilon - 1}{4\pi} \right) E \quad (2)$$

[†] Part of the special issue “David Chandler Festschrift”.

* Corresponding author. E-mail: rasaiah@maine.edu.

[‡] Department of Physics and Astronomy.[§] Current address: Institute of Physical Science and Technology, University of Maryland, College Park, MD 20742.^{||} Department of Chemistry.

and integrating it with respect to E , one finds that the relative change in the density of the fluid is proportional to the square of the field E

$$\frac{\rho(E) - \rho(0)}{\rho(0)} = \frac{\kappa_T^0 \rho(0)}{8\pi} \frac{\partial \epsilon}{\partial \rho(0)} E^2 \quad (3)$$

with $\kappa_T = \kappa_T^0 + O(E^2)$ and $\partial \epsilon / \partial \rho = \partial \epsilon / \partial \rho(0) + O(E^2)$. This well-known expression for electrostriction, discussed by Kirkwood and Oppenheim³⁶ and Frank,³⁵ can also be derived from a molecular theory^{38,39} and applies only at low electric fields to the first order in E^2 . The density changes with the square of the electric field, and the sign of this change is determined by the sign of $\partial \epsilon / \partial \rho(0)$. From experimental studies⁴⁰ of water at 25 °C, $\partial \ln \epsilon / \partial \ln P = 4.7 \times 10^{-5}$, where P is the pressure. Because $\partial \epsilon / \partial \rho = (1/\rho \kappa_T) (\partial \epsilon / \partial P)$ and κ_T is positive, we conclude that $\partial \epsilon / \partial \rho(0)$ is also positive for a macroscopic sample of water at 25 °C and the density should initially increase with the applied electric field.

In this study, we find just the opposite effect when an electric field is applied to a narrow water sample between two graphene plates open to a water reservoir. The field acts only on the water between the plates. In addition, we observe spontaneous evaporation of water between large graphene plates at a separation of 9.5 Å at zero field, when the plate–water interaction is tuned to be more repulsive than the “normal” carbon–water interaction. Evaporation is further enhanced by applying an electric field between the plates. The zero-field effect disappears for smaller plates, signaling a crossover with decreasing plate size, but the density depletion with the presence of an electric field remains.

We note that a statistical mechanical theory of electrostriction has been developed using integral equation approximations for the wall–particle (in this case water) correlation function. The hypernetted chain approximation for the wall–particle closure also predicts electrostriction proportional to the square of the electric field, but with a different positive proportionality constant.^{41,42} Comparison with the thermodynamic theory, after addition of the bridge diagram of $O(E^2)$ to the wall–particle correlation functions, leads to a differential equation for the dielectric constant whose solution is an exact expression for the dielectric constant⁴³ first proposed by Ramshaw.⁴⁴ The integral equation theory, however, is not directly relevant to the present study because it applies to a dipolar fluid that is infinitely far away from a charged wall and not to a fluid between plates at a finite distance apart. In a different sense, this is also true of the thermodynamic theory of electrostriction discussed above because surface effects are ignored.

The apparent contradiction with the bulk thermodynamics of electrostriction suggests that the water between the plates considered in our study may be at or near a metastable region. The free energy of water between or near such surfaces in the absence of an electric field has been discussed theoretically by Chandler and his group^{15,45–47} in the context of hydrophobic solvation and dewetting. The dynamics of water evaporation between plates has been studied by Lum and Luzar²¹ and by Luzar et al.^{23–25,28}

The critical distance D_c below which water between plates of lateral dimension L is thermodynamically unstable^{15,21} is given by

$$D_c \sim 2\Delta\gamma/(\rho\Delta\mu + 4\gamma/L) \quad (4)$$

This could be as large as 1024 nm for infinitely large plates under ambient conditions, assuming a contact angle θ_c of 135°.

Here $\Delta\gamma = -\gamma \cos \theta_c$, γ is the surface tension of the free liquid, ρ is the number density of the liquid, and $\Delta\mu$ is the difference in chemical potentials between liquid and vapor. However, liquid water can coexist in a metastable state with a surface vapor film between large hydrophobic plates at much smaller separations. Lum et al.¹⁵ estimate this limit of metastability to be about 5 nm for water between hard walls at room temperature and a pressure of 1 atm. Grand canonical Monte Carlo (GCMC) simulations by Bratko et al.,¹ at ambient conditions, suggest that the limit of metastability (spinodal region) over practical simulation times occurs at separations of 1.27 nm for weakly attractive hydrocarbon-like plates with about three intervening water molecule layers when the plate dimensions L are much larger than their separation. Smaller plates shift the critical distance for thermodynamic stability to lower values when the plate size dominates the denominator in eq 4. Spontaneous evaporation occurs at plate distances below the metastable limit.²⁵ This was seen in GCMC simulations²² of water between hard walls and in MD simulations¹⁹ of two hydrophobic ellipsoidal surfaces immersed in water. More recently,²⁰ the collapse of ellipsoidal particles induced by dewetting and the evaporation of water between plates²⁵ have been observed in MD simulations.

Equation 4 reduces to the Kelvin equation $D \sim 2\Delta\gamma/\rho\Delta\mu$ in the limit $L \rightarrow \infty$. Dzubiella and Hansen⁴⁸ have generalized this to include the effect of an electric field in studying the stability of charged colloids and find that it suppresses water expulsion. This is also the opposite of what we observe for water between plates.

II. Simulation Details

The package DL_POLY⁴⁹ was used to conduct constant-pressure and -temperature MD simulations with the Nosé–Hoover algorithm. Simulations were performed with SPC/E water⁵⁰ at pressure $P = 1$ bar, temperature $T = 300$ K, and time step = 1 fs. Systems of two different sizes were investigated. The smaller one had 500 water molecules in a cubical simulation cell that was about 25 Å on each side. Embedded in this cell, parallel to the X – Y plane and symmetrically along the Z axis, were two plates of dimensions 9.8×9.2 Å with 45 atoms in a graphene structure. The plate separation D was 8.0 Å. The larger system had 1372 water molecules in a cubical cell that was approximately 35 Å on each side. These plates (Figure 1) of dimensions 17.7×17.2 Å had 133 atoms in the same graphene structure. Simulations were carried out at plate separations D of 8.0 (data not shown), 9.5, and 16.4 Å.

The atoms on the plates interacted with the oxygen atoms in the water molecules via a Lennard-Jones potential. Two different sets of parameters for the effective size σ and well depth ϵ were studied. The first had $\sigma = 3.283$ Å and $\epsilon = 0.000$ 28 kcal/mol. This mimics a hard wall at the position of each plate because ϵ is small, finite, and positive. The second had the same σ value with $\epsilon = 0.116$ kcal/mol. This potential corresponds to the standard C–O interaction obtained from the Lorentz–Bertholet mixing rules applied to carbon atoms in graphite and oxygen atoms in water, and it is more hydrophilic and less hydrophobic than the former. We refer to these sets as “hard-wall-like” and “normal” C–O potentials. In keeping with common usage, both of these may be termed hydrophobic potentials, but we use them only in a relative sense. We have also carried out a few simulations for a soft repulsive potential between the atoms of the graphene sheet and water in which the attractive dispersion term in the Lennard-Jones potential is suppressed by setting it equal to zero.

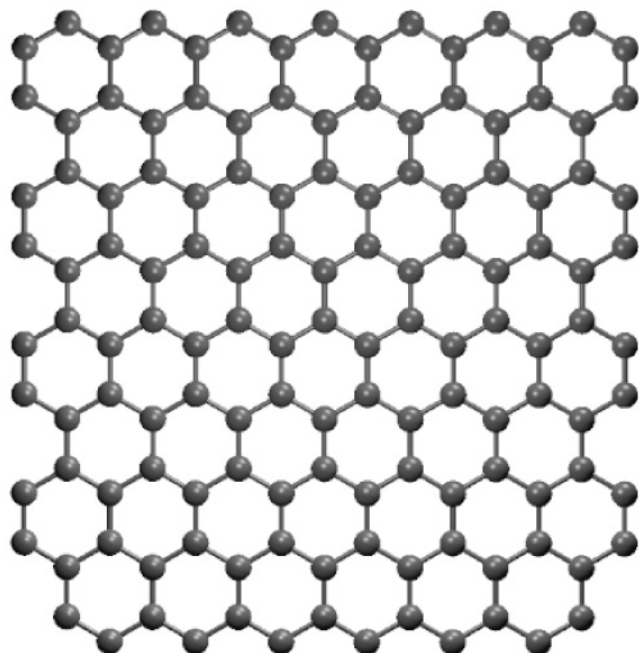


Figure 1. Large graphite plate with 133 carbon atoms and dimensions 17.7×17.2 Å.

The region between the plates is thus an open system that is free to exchange matter and energy with the surrounding bath. To study the effect of an external electric field on a fluid in an open system, a uniform field ranging from 0 to 8.68 V/nm was turned on perpendicular to the plates along the Z axis and acted only on the water between the plates. To place this in perspective, we note that a surface charge density of one electronic charge per 1000 Å² corresponds to a field of 1.8 V/nm. Periodic boundary conditions were applied with Ewald sums for the long-range electrostatic interactions. Equilibration runs were at least 500 ps long, with the time step gradually increasing from 0.1 to 1 fs. After equilibration, data were collected for 300–500 ps for each system. Temperature fluctuations were found to have standard deviations of ~ 4.66 K, irrespective of the plate–water interaction or the applied field. Pressure fluctuations were insensitive to the plate–water interaction but increased with the field strength. The standard deviations were ~ 0.3 bar at $E = 0$ V/nm and ~ 1.2 bar at $E = 8.68$ V/nm. These very large pressure fluctuations can be attributed to the low compressibility of water.

MD trajectories were saved every 50 steps for further analysis. Density profiles $\langle \rho(z, E) \rangle = \langle N(z, \Delta z, t) \rangle / A \Delta z$ were calculated from histograms of the number of water molecules along the Z axis, where $N(z, \Delta z, t)$ is the number of water molecules at time t in a bin of width Δz at position z along the Z axis and A is the area of each plate. Similar profiles were calculated for the z component of the molecular dipole moment, $\langle \mu_z(z, E) \rangle = \langle \sum_{i=1}^{N(t)} \mu_{z,i}(z, \Delta z, t) / N(t) \rangle$, and for the component of the molecular dipole moment parallel to the plates. The polarization density was also calculated from $\langle P_z(z, E) \rangle = \langle \sum_{i=1}^{N(t)} \mu_{z,i}(z, \Delta z, t) \rangle / A \Delta z$, which is also equal to $\langle \rho(z, t) \mu_z(z, \Delta z, t) \rangle$.

III. Results and Discussion

1. Larger Plates of 17.7×17.2 Å. Figure 2 shows snapshots of the large equilibrated system with “hard-wall-like” plates at a separation of 16.4 Å with and without an external electric field between the plates, along the Z axis. The polarization of the water by the external field along with a reduction in the

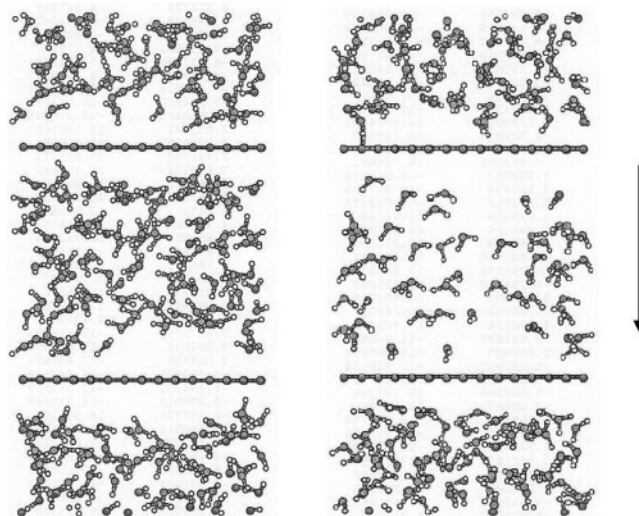


Figure 2. Snapshot of the larger system with “hard walls” at zero field (left) and an electric field of $E = 4.34$ V/nm (right). The field is directed along the Z axis, as indicated by the arrow. Only water molecules between or directly above and below the plates are shown for clarity.

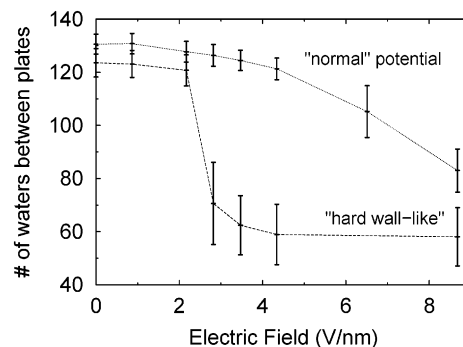


Figure 3. Number of water molecules between the plates as a function of the applied electric field for the large system for the two potentials studied. The plates are 16.4 Å apart, and the volume between them is 304.4 Å³.

density can be clearly seen. In Figure 3, we plot the number of water molecules between the plates, averaged over 300–500 ps, as a function of the applied field. The steep drop in this number when the field strength exceeds ~ 2.2 V/nm along with the nearly two-state behavior suggests a liquid-to-vapor-like phase transition. Density profiles for different field strengths and plate separations (16.4 and 9.5 Å) are shown in Figure 4.

At zero field, with a plate separation of 16.4 Å (Figure 4a), the water between the plates is layered with four peaks visible at densities close to that of the bulk liquid, 1 gm/cm³. Water on either side of the plates is also perturbed, with two peaks visible in the density profile on each side. Applying an electric field to the water between the plates has the unexpected and dramatic effect of reducing the density between the plates gradually and then rapidly at fields just beyond 2.17 V/nm. At this point, the layers next to the plates are more sharply defined, with merging of the layers in between. At a slightly larger field strength of 2.82 V/nm, the intervening fluid has a greatly reduced density, with the layers immediately next to the plates still well-defined but showing a marked asymmetry, reflecting the charge asymmetry of the oriented water molecules in the layers next to the plates. At or near this field strength, the fluid between the plates is in transition to a lower-density vaporlike phase accompanied by large density fluctuations, as seen from the error bars in Figure 3. Long-lived density fluctuations in

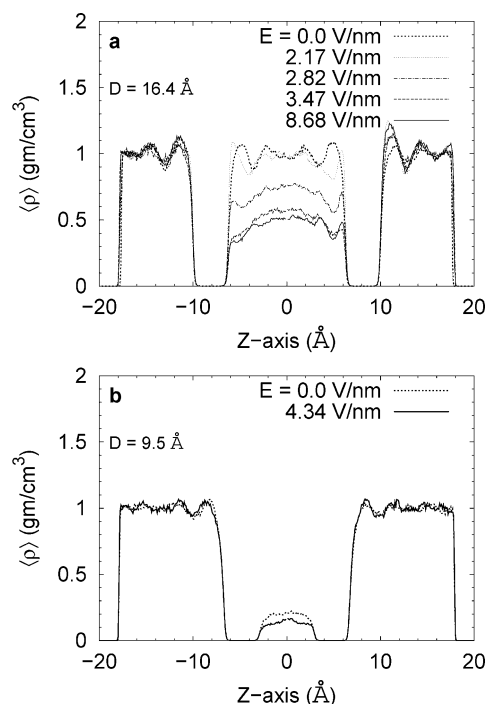


Figure 4. Density profiles for the larger system (1372 water molecules) with “hard walls” of dimensions 17.7×17.2 Å at separations of (a) 16.4 Å and (b) 9.5 Å.

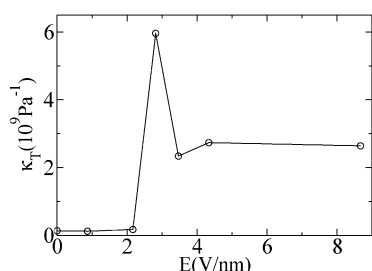


Figure 5. Compressibility of water in the region between “hard-wall-like” plates at 300 K calculated from the particle fluctuations in this region at a constant volume.

confined water have also been observed earlier by Bratko et al., but in the absence of an electric field.¹ The compressibility of the fluid between the plates, calculated from fluctuations in the number of water molecules ($\langle N^2 \rangle - \langle N \rangle^2$), shows a maximum at a field of 2.82 V/nm (Figure 5), resembling a liquid–vapor phase transition. The water density decreases to about 0.5 gm/cm³ at a field of 3.47 V/nm, with only a further small decrease as the field strength increases to 8.68 V/nm. At these high fields, the water between the plates, which is open to a reservoir, becomes more vaporlike, and the density remains constant with increasing field (Figure 3). The water in the region immediately outside the plates is insensitive to the electric field (Figure 4a).

The fluctuations in the number of water molecules as a function of time for differing electric fields are illustrated in Figure 6. At a field of 2.82 V/nm, which coincides with the observed shift in the average density, the number of water molecules (dark curve in Figure 6) changes between the average number observed at low (0.87 V/nm) and high (4.34 V/nm) fields. Our simulations over equilibrated times of 500 ps are too short to provide a more detailed picture of the dynamics of these transitions.

These calculations for water between large plates at a separation of 16.4 Å were repeated⁵¹ using only the repulsive part of the Lennard-Jones potential between the plate atoms and

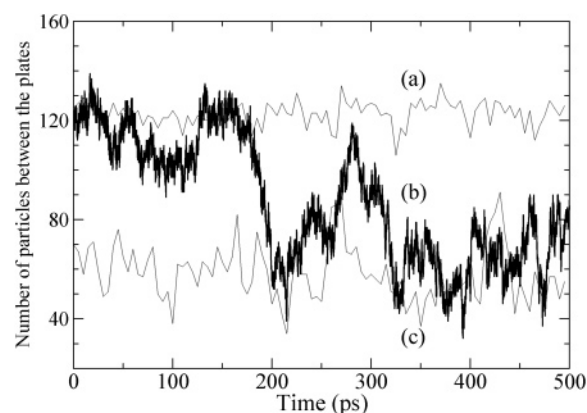


Figure 6. Time dependence of water molecule population in the region between “hard-wall-like” plates at a separation of 16.4 Å and 300 K at electric fields of (a) 0.87 V/nm, (b) 2.82 V/nm, and (c) 4.34 V/nm. To improve the clarity of the figure, the time interval between data points for parts a and c was chosen as 5 ps, while that for part b was 0.05 ps.

the oxygen of the water molecules but with the same σ and ϵ as the “normal” C–O potentials. On average, slightly fewer water molecules were observed between the plates, but the fluctuations and density depletion in the presence of an electric field are similar to what we observe for water between plates with “hard-wall-like” potentials.

When the separation between the plates is reduced to 9.5 Å, spontaneous evaporation of water between “hard-wall-like” plates at zero field occurs, which is shown in Figure 4b. The fluid between the plates is structureless, with a greatly reduced density of ~ 0.2 gm/cm³ at this separation. Evaporation of water between closely spaced hydrophobic surfaces has been reported earlier in MD¹⁹ and Monte Carlo^{1,22,23,25} simulations. The system in Figure 4b is comparable to the ones studied by Wallqvist and Berne¹⁹ and Huang et al.,²⁰ with plates of similar size and at the same center-to-center separation. We observe a further reduction in the density when an electric field is applied between the plates. To our knowledge, this has not been reported before.

We next consider our simulations of water between plates with the “normal” C–O potential corresponding to the regular C–O interaction. Figure 3 shows that the number of water molecules between the plates again decreases with increasing field strength, as with the more hydrophobic “hard-wall-like” plates. However, while the latter had a phase-transition-like character between liquid- and vaporlike phases, the density change with the presence of an electric field is less abrupt for the more attractive and less hydrophobic (“normal” C–O potential) plates. The density profiles (Figure 7) show that the water between these plates retains its layering at all fields, with the density in each layer close to or exceeding the density of bulk water, 1 gm/cm³. The stronger interaction between the plate carbons and the water molecules corresponds to a smaller contact angle than that for the “hard-wall-like” potential. This prevents field-induced evaporation and leads to more sharply defined water layers between and immediately outside of the plates. The water density in the first layers next to the plates exceeds 3 gm/cm³ at zero field. Correspondingly, the first minima next to the plates are deep, ~ 0.5 gm/cm³. At zero field, the water between the plates exists in four well-defined layers. With an increasing field strength, the number of layers also increases; there are five at fields of 2.17 and 4.34 V/nm and six at the highest field of 8.68 V/nm. As the electric field increases, an asymmetry develops in the density profile that is due to the charge asymmetry of the water molecule, as reported above for “hard-wall-like” plates.

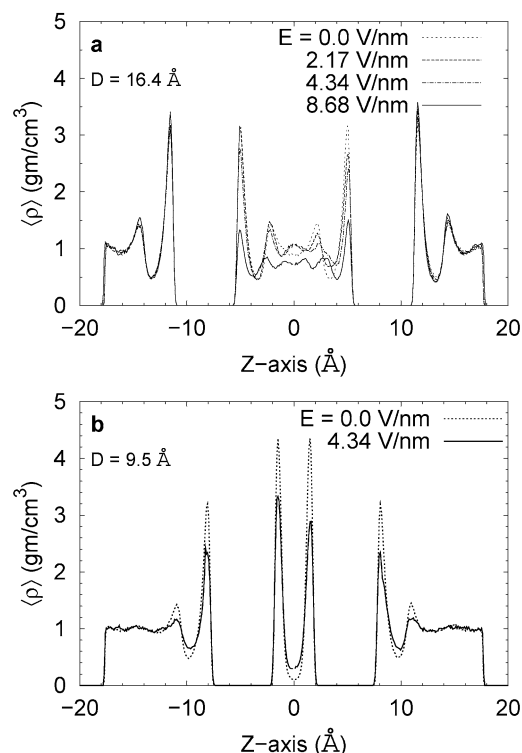


Figure 7. Density profiles for the larger system (1372 water molecules) between walls with “normal” C–O potentials. The plates have dimensions of 17.7×17.2 Å and are at separations of (a) 16.4 Å and (b) 9.5 Å.

The polarization density profiles (not shown) of the water between the plates were seen to be in phase with the density profiles. Figure 8a shows the polarization density in the middle layer ($z = 0$) between the plates as a function of the field for both the “normal” C–O and “hard-wall-like” plates. This is calculated directly in our simulations and compared with the approximation $\langle P_z(z, E) \rangle \approx \langle \rho(z, E) \rangle \langle \mu_z(z, E) \rangle^{52}$ in the same figure. The two are virtually identical for both types of plates, showing that the approximation is excellent. The same approximation holds for a Stockmayer fluid in a closed system in the presence of an electric field that was shown in studies by one of us with Lee and Hubbard.⁵² Figure 8b displays the local density $\langle \rho(z, E) \rangle$ and the average z component of the molecular dipole moment of water $\langle \mu_z \rangle$ in the middle layer, both of which are used in the above approximation. The density variation with electric field follows nearly the same trend as that of the total number of water molecules in the region between the plates (Figure 3), while the z component of the dipole moment is the same for both plate types and is well represented by the Debye theory of ideal dipoles with $\langle \mu_z \rangle = \mu L(y)$, where $L(y)$ is the Langevin function and $y = (\mu|E|/k_B T)$, in which k_B is Boltzmann’s constant, T is the temperature in degrees Kelvin, and μ ($=2.35$ D) is the dipole moment of an SPC/E water molecule. This behavior was also observed earlier for a Stockmayer fluid in a closed system.⁵²

The orientational polarization of the water molecules by an electric field affects their spatial correlation. We investigated this by calculating the pair correlation function between oxygen atoms of distinct water molecules in a 1 Å thick layer halfway between “hard-wall-like” plates at zero field and a field of 4.34 V/nm. Figure 9 shows that the height of the first nearest-neighbor peak is sharply reduced when a field of 4.34 V/nm is applied and is accompanied by a wider and enhanced distribution of molecules at larger distances.

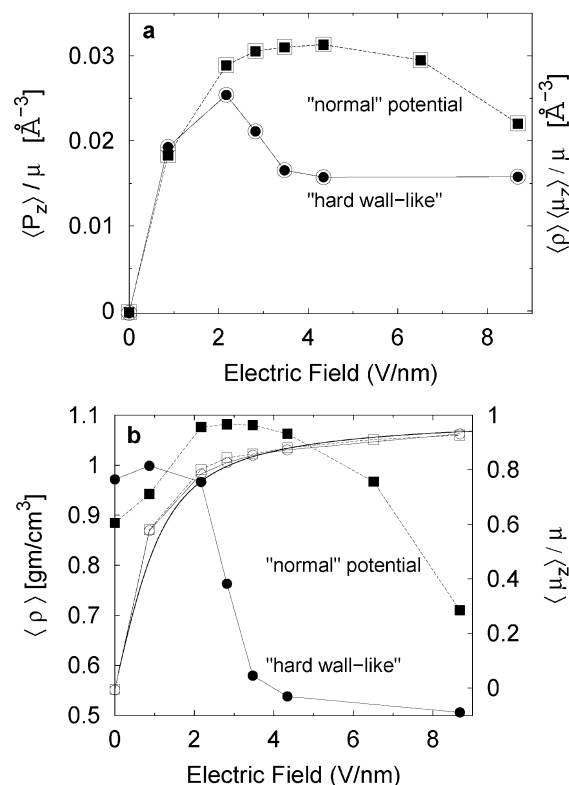


Figure 8. (a) Polarization densities at $z = 0$. (b) Density ρ and $\langle \mu_z \rangle$ in the middle layer for both wall–particle potentials. Solid symbols refer to the left ordinate, and open symbols refer to the right ordinate. The smooth curve in part b is the prediction of the Debye–Langevin equation for a dipolar fluid in an electric field. Circles apply to the “hard-wall-like” potential and squares to the “normal” potential.

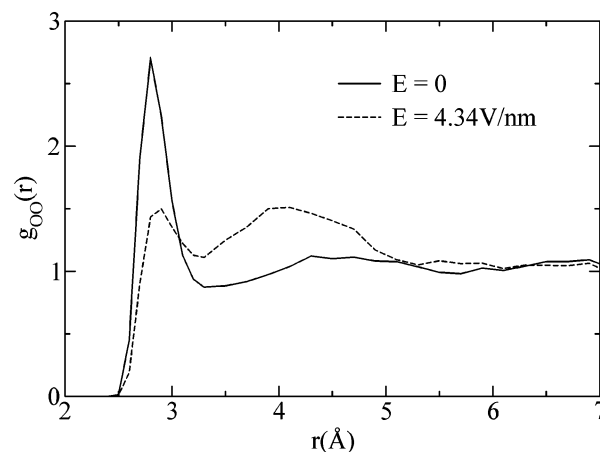


Figure 9. Pair correlation function of oxygen atoms on water molecules in the middle layer of thickness, 1 Å between “hard-wall-like” plates of dimension 17.7×17.2 Å at zero field and at a field of 4.35 V/nm.

2. Smaller Plates of 9.8×9.2 Å. Smaller “hard-wall-like” plates have a qualitatively different effect on the interstitial fluid. Figure 10 displays the density profiles, averaged over 300 ps, for the smaller system of 500 water molecules with parallel plates immersed at a separation of 8.0 Å. These plates have dimensions of 9.8×9.2 Å and, have less than one-third the surface area of the larger plates discussed above. At zero field, two well-defined water layers are observed between the plates with a local density of ~ 1.5 gm/cm³, in contrast to the larger plates at the same separation, which peak at a density of ~ 0.1 gm/cm³ (data not shown). The local density of water in the layers between the smaller “hard-wall-like” plates is thus greater

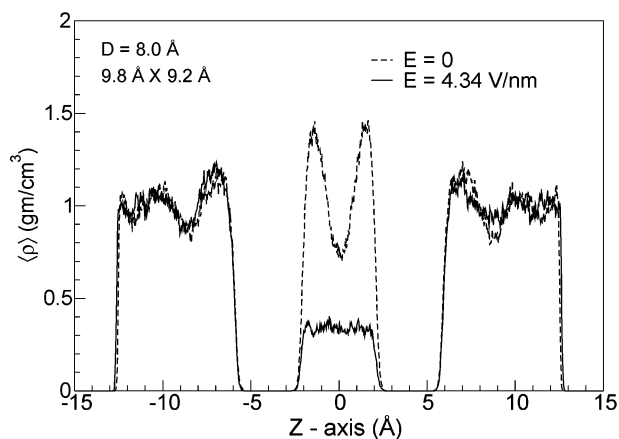


Figure 10. Density profiles for the box of 500 water molecules with embedded “hard walls”, with and without an applied electric field. Profiles are averaged over 300 ps. The plates have dimensions of 9.8×9.2 Å and are positioned at ± 4.0 Å along the Z axis.

than the water density in the reservoir, unlike the density lowering due to the spontaneous evaporation of water between larger plates at a 9.4 Å separation. This signals a crossover as the plate dimension L decreases, when the second term in the denominator of eq 4 becomes dominant, and the critical distance D_c , at which the intervening fluid is metastable, becomes smaller. It is like the crossover associated with the formation of a liquid–vapor interface as the size of a nonpolar solute increases.⁴⁶

When an electric field is applied between the plates, we again see a transition to a vapor phase with an average density of ~ 0.3 gm/cm³ and a complete loss of layering. With field strengths of 0 and 4.34 V/nm, there are on average ~ 14 and ~ 4 water molecules, respectively, between the plates.

IV. Conclusions

We have studied the behavior of thin films of water between plates of different hydrophobicity by MD simulation, both in the presence and in the absence of an electric field and at different plate separations. The contrast between our results and the bulk thermodynamics prediction³⁶ of an increase in density of a dipolar fluid with the presence of an electric field in an open system is striking. The thermodynamic theory treats the fluid as a continuum dielectric, neglecting boundary effects associated with the plate–particle interactions at the interfaces. The increase in density with the presence of an electric field is commonly described as “electrostriction”. We observe just the opposite behavior in our simulations; an electric field decreases the density of a water film between plates and, moreover, enhances its evaporation, when it occurs, at small plate separations in the absence of a field. The extent of water depletion in an electric field depends critically on the plate–water interaction. A strongly repulsive, or more hydrophobic, plate–water potential is more effective in expelling water when an electric field is applied and promotes a sudden drop in the number of water molecules between the plates at a critical value of the electric field. This is accompanied by large density fluctuations and a sharp rise in the compressibility, resembling a liquid–vapor phase transition. We also observe a crossover to spontaneous evaporation of water between “hard-wall-like” hydrophobic plates at zero field as the plate size increases when their separation is small. This surface-induced evaporation is further enhanced by an electric field.

These observations are related not only to the special properties of water, characterized by hydrogen bonding and

dewetting at large hydrophobic surfaces, but also to the metastability or instability of thin films between finite-sized plates at separations below the critical distance for thermodynamic stability.^{14,15,25} This has interesting implications for the behavior of narrow films of water between surfaces and membranes in real physical and biological systems.⁵³

Our simulations suggest that the free energy barrier for capillary evaporation between narrowly separated plates is reduced by the application of an electric field. A qualitative explanation of water depletion between such plates, when open to a reservoir, follows from a consideration of its orientation polarization in an electric field. At zero field, the average component of the dipole moment perpendicular to the confining plates, $\langle u_z \rangle$, and in the middle layers of water between the plates is also zero. The intervening fluid is polarized as the field between the plates increases, and at the highest fields investigated here, the water molecules are almost completely oriented with the field. The mutual repulsion between the water dipoles in the same layer promotes fluid transfer from the region between the plates to the surrounding bath. Evaporation is enhanced when the fluid is metastable and the plate–water interaction is strongly repulsive. This interpretation is consistent with our calculations of the “in-plane” distribution functions of water (Figure 9) near the middle of the fluid film between large “hard-wall-like” plates.

Water molecules near a hard wall reorient spontaneously to maximize hydrogen bonding.^{13,54} When this occurs, the preferred orientation near the wall could be disrupted by an external electric field and modified by changing the wall–particle potential to include van der Waals or other interactions. At very large plate separations, the surface contributions to the thermodynamics of the fluid are less evident, and its behavior approaches that of a bulk fluid in an electric field. A quantitative theory of electric field effects on narrowly confined water or polar fluids between plates that takes into account surface effects including reorganization and polarization near the interface has yet to be developed.

Acknowledgment. We thank Steven Fortune for his assistance and interest, George Stell, Dusan Bratko, Alenka Luzar, and Ruth Lynden-Bell for helpful discussions, and the University of Maine Supercomputing Center for computing time. This research was supported by a National Science Foundation Grant (CHE 9981336) to J.C.R.

References and Notes

- (1) Bratko, D.; Curtis, R. A.; Blanch, H. W.; Prausnitz, J. M. *J. Chem. Phys.* **2001**, *115*, 3873.
- (2) Horn, R. G.; Israelachvili, J. N. *J. Chem. Phys.* **1981**, *75*, 1400.
- (3) Israelachvili, J. N. *Acc. Chem. Res.* **1987**, *20*, 415.
- (4) Israelachvili, J. N. *Intermolecular and Surface Forces*; Academic Press: New York, 1992.
- (5) Vaitheeswaran, S.; Yin, H.; Rasaiah, J. C.; Hummer, G. *Proc. Natl. Acad. Sci. USA* **2004**, *101*, 17002.
- (6) Hummer, G.; Rasaiah, J. C.; Noworyta, J. P. *Nature* **2001**, *414*, 188.
- (7) Waghe, A.; Rasaiah, J. C.; Hummer, G. *J. Chem. Phys.* **2002**, *117*, 10789.
- (8) Allen, R.; Melchionna, S.; Hansen, J. P. *Phys. Rev. Lett.* **2002**, *89*, 175502.
- (9) Allen, R.; Hansen, J. P.; Melchionna, S. *J. Chem. Phys.* **2003**, *119*, 3905.
- (10) Maibaum, L.; Chandler, D. *J. Phys. Chem. B* **2003**, *107*, 1189.
- (11) Vaitheeswaran, S.; Rasaiah, J. C.; Hummer, G. *J. Chem. Phys.* **2004**, *121*, 7955.
- (12) Zhou, X.; Li, C.-Q.; Iwamoto, M. *J. Chem. Phys.* **2004**, *121*, 7996.
- (13) Stillinger, F. H. *J. Solution Chem.* **1973**, *2*, 141.
- (14) Lum, K.; Chandler, D. *Int. J. Thermophys.* **1998**, *19*, 845.

- (15) Lum, K.; Chandler, D.; Weeks, J. D. *J. Phys. Chem. B* **1999**, *103*, 4570.
- (16) Truskett, T. M.; Debenedetti, P. G.; Torquato, S. *J. Chem. Phys.* **2001**, *114* (5), 2401–2418.
- (17) Lee, C. Y.; McCammon, J. A.; Rossky, P. J. *J. Chem. Phys.* **1984**, *80*, 4448.
- (18) Lee, S. H.; Rossky, P. J. *J. Chem. Phys.* **1994**, *100*, 3334.
- (19) Wallqvist, A.; Berne, B. J. *J. Phys. Chem.* **1995**, *99*, 2893.
- (20) Huang, X.; Margulis, C. J.; Berne, B. J. *Proc. Natl. Acad. Sci. U.S.A.* **2003**, *100* (21), 11953–11958.
- (21) Lum, K.; Luzar, A. *Phys. Rev. E: Stat. Phys., Plasmas, Fluids, Relat. Interdiscip. Top.* **1997**, *56*, 6283.
- (22) Luzar, A.; Bratko, D.; Blum, L. J. *J. Chem. Phys.* **1987**, *86*, 2955.
- (23) Luzar, A.; Leung, K. *J. Chem. Phys.* **2000**, *113*, 5836.
- (24) Leung, K.; Luzar, A. *J. Chem. Phys.* **2000**, *113*, 5845.
- (25) Leung, K.; Luzar, A.; Bratko, D. *Phys. Rev. Lett.* **2003**, *90*, 65502.
- (26) Spohr, E.; Trokhymchuk, A.; Henderson, D. *J. Electroanal. Chem.* **1998**, *450*, 281.
- (27) Hayashi, T.; Pertsin, A. J.; Grunze, M. *J. Chem. Phys.* **2002**, *117*, 6271–6280.
- (28) Luzar, A. *J. Phys. Chem. B* **2004**, in press.
- (29) Christenson, H. K.; Claesson, P. M. *Adv. Colloid Interface Sci.* **2001**, *91*, 3915.
- (30) Svischev, I. M.; Kusalik, P. G. *Phys. Rev. Lett.* **1994**, *73*, 975.
- (31) Xia, X.; Berkowitz, M. L. *Phys. Rev. Lett.* **1995**, *74*, 3193.
- (32) Yeh, I. C.; Berkowitz, M. L. *J. Chem. Phys.* **1999**, *111*, 3155.
- (33) Yeh, I. C.; Berkowitz, M. L. *J. Chem. Phys.* **2000**, *112*, 10491.
- (34) Zhu, S.-B.; Robinson, G. W. *J. Chem. Phys.* **1991**, *94*, 1403.
- (35) Frank, H. S. *J. Chem. Phys.* **1955**, *23*, 2023.
- (36) Kirkwood, J.; Oppenheim, I. *Chemical Thermodynamics*; McGraw-Hill: New York, 1961.
- (37) Blum, L.; Rasaiah, J. C.; Vericat, F. *J. Chem. Phys.* **1983**, *78*, 3233.
- (38) Carnie, S.; Stell, G. *J. Chem. Phys.* **1980**, *77*, 1017.
- (39) Høye, J. S.; Stell, G. *J. Chem. Phys.* **1981**, *75*, 3559.
- (40) Owen, B. B.; Miller, R. C.; Milnes, C. E.; Cogan, H. *J. Phys. Chem.* **1961**, *65*, 2065.
- (41) Rasaiah, J. C.; Isbister, D. J.; Stell, G. *J. Chem. Phys.* **1981**, *75*, 4707.
- (42) Rasaiah, J. C.; Isbister, D. J.; Stell, G. *Chem. Phys. Lett.* **1981**, *79*, 189.
- (43) Rasaiah, J. C. *J. Chem. Phys.* **1982**, *77*, 5710.
- (44) Ramshaw, J. *J. Chem. Phys.* **1972**, *57*, 2684.
- (45) Huang, D. M.; Geissler, P.; Chandler, D. *J. Phys. Chem. B* **2001**, *105*, 6704.
- (46) Huang, D. M.; Chandler, D. *J. Phys. Chem. B* **2002**, *106*, 2047–2053.
- (47) Huang, D. M.; Chandler, D. *Proc. Natl. Acad. Sci. U.S.A.* **2000**, *97*, 8324.
- (48) Dzubiella, J.; Hansen, J.-P. *J. Chem. Phys.* **2003**, *119* (23), 12049–12052.
- (49) Smith, W.; Forester, T. R. *J. Mol. Graphics* **1996**, *14*, 136.
- (50) Berendsen, H. J. C.; Grigera, J. R.; Straatsma, T. P. *J. Phys. Chem.* **1987**, *91*, 6269.
- (51) Yin, H.; Fortune, S.; Rasaiah, J. C. Unpublished work, 2004, Department of Chemistry, University of Maine.
- (52) Lee, S. H.; Rasaiah, J. C.; Hubbard, J. B. *J. Chem. Phys.* **1986**, *85*, 5232.
- (53) Zhou, R.; Huang, X.; Margulis, C. J.; Berne, B. J. *Science* **2004**, *305*, 1605–1609.
- (54) Luzar, A.; Svetina, S.; Zeks, B. *J. Chem. Phys.* **1985**, *82*, 5146.